Nuclear Science and Techniques (2023) 34:107
https://doi.org/10.1007/s41365-023-01252-w

Design and comparison of hybrid multi-bend achromat lattices for HALF storage ring

Peng-Hui Yang[1] · Gang-Wen Liu[1] · Jian-Hao Xu[1] · Wei-Wei Li[1] · Tian-Long He[1] · Zheng-He Bai[1]

Received: 19 July 2022 / Revised: 8 March 2023 / Accepted: 12 April 2023 / Published online: 24 July 2023

Abstract
The Hefei Advanced Light Facility (HALF) proposed by the National Synchrotron Radiation Laboratory is a green-field vacuum ultraviolet and soft X-ray diffraction-limited storage ring light source with a beam energy of 2.2 GeV and emittance goal of less than 100 pm rad. Inspired by the ESRF-EBS hybrid multi-bend achromat (HMBA), SLS-2, and Diamond-II lattices, we have proposed and designed a modified H6BA lattice as the baseline lattice of the HALF storage ring with 20 identical cells and a natural emittance of approximately 86 pm rad. In this paper, three other types of HMBA lattices including two H7BA lattices and a H6BA lattice are designed for HALF with the same number of cells. The main storage ring properties of these four HMBA lattices are compared. Because the intra-beam scattering (IBS) effect is significant in the HALF storage ring, we calculate and compare the equilibrium emittances of the four lattices with IBS included. These comparisons show that the present modified H6BA lattice, which has a relatively low equilibrium emittance and more straight sections, is preferred for the HALF storage ring after a comprehensive consideration.

Keywords Hefei advanced light facility · Lattice design · Hybrid MBA lattice · Intra-beam scattering

1 Introduction

The Hefei Light Source (HLS) located at the National Synchrotron Radiation Laboratory (NSRL) is a second-generation vacuum ultraviolet (VUV) and soft X-ray synchrotron light source that has been in operation for approximately 30 years. HLS has been upgraded and improved in recent years to enhance its performance [1–4]. The beam energy of the linac was increased from 200 to 800 MeV to enable full-energy injection for top-up operation. The natural emittance was reduced from approximately 160 to 36 nm rad and the beam current increased from 300 to 400 mA. In addition, a fourth-harmonic radio frequency (RF) cavity was installed in the HLS storage ring to increase the beam lifetime and reduce beam instability. There are currently five beamlines from insertion devices (IDs) and five from bending magnets (bends). An ultralow-emittance lattice was recently designed to reduce the natural emittance by approximately one order of magnitude to 3.9 nm rad for the future development of HLS [5]. Although efforts have been made to improve the performance of HLS, the ID radiation brightness and number of straight sections remain limited.

Today, fourth-generation storage ring light sources, i.e., the so-called diffraction-limited storage rings (DLSRs) [6], are being developed rapidly worldwide. Examples include MAX IV [7], ESRF-EBS [8], Sirius [9], APS-U [10], HEPS [11], SLS-2 [12], ALS-U [13] and Elettra 2.0 [14]. The emittances of these DLSRs can reach as low as hundreds or even tens of pm rad and the ID radiation brightness is about 1–2 orders of magnitude higher than that of third-generation light sources. To maintain competitiveness, NSRL has also proposed a new soft X-ray and VUV DLSR called the Hefei Advanced Light Facility (HALF) [15], which was approved recently. The beam energy of the HALF storage ring is 2.2

This work was supported by the Fundamental Research Funds for the Central Universities (No. WK2310000107), the National Key Research and Development Program of China (No. 2016YFA0402000) and National Natural Science Foundation of China (Nos. 12205299, 11875259, 12105284).

✉ Tian-Long He
htlong@ustc.edu.cn

✉ Zheng-He Bai
baizhe@ustc.edu.cn

[1] National Synchrotron Radiation Laboratory, University of Science and Technology of China, Hefei 230029, China

GeV and the natural emittance goal is less than 100 pm rad with 20 lattice cells.

Because the natural emittance of the storage ring is inversely proportional to the third power of the number of bends, multi-bend achromat (MBA) lattices [16] are used in DLSR designs. The hybrid MBA (HMBA) lattice [17], which was proposed by ESRF-EBS, has been adopted or imitated by APS-U [10], HEPS [11], PETRA-IV [18], ALS-U [19], Diamond-II [20], SSRF-U [21], SAPS [22], and other DSLRs owing to its advantages, which include a relatively large on-momentum dynamic aperture (DA), relatively weak sextupole strengths, and compact magnet layout. In a typical H7BA lattice, four longitudinal gradient bends (LGBs) with dipole fields adapted to dispersion variation are employed on both sides of the lattice to help reduce emittance. A pair of dispersion bumps is introduced between the LGBs to reduce the strength of the sextupoles located therein for chromaticity correction. In addition, the horizontal and vertical phase advances between the dispersion bumps are approximately $(3\pi, \pi)$ such that the main nonlinear effects caused by the sextupoles can be mitigated within one lattice cell. In the middle of the lattice cell, three combined-function bend unit cells with relatively strong quadrupole gradients and relatively low dispersion are employed to efficiently lower the emittance.

Modified versions of the HMBA lattice have been proposed to further enhance the performance of the light source. The emittance of the APS-U H7BA lattice is reduced by approximately 40% when three families of reverse bends (RBs) are employed [10]. To provide more straight sections, a modified H6BA lattice was proposed for Diamond-II in which the central bend of the H7BA lattice is replaced by a mid-straight section [20]. The HEPS lattice is a super-period H7BA lattice with high- and low-beta straight sections, which enhances the ID radiation brightness in the low-beta straight line, and a LGB is used in the central bend as a superior bend radiation source [11]. In addition, other modified HMBA lattices have different advantages. For example, the H10BA lattice has a lower emittance [23] while all the main bends in compact HMBA lattices are combined-function bends to save space [24, 25].

To reduce both the damping times and emittance, HALF has also proposed and designed a modified H6BA lattice [15], which combines the merits of the ESRF-EBS HMBA and SLS-2 LGB/RB unit lattices and employs an additional mid-straight section similar to that in the Diamond-II lattice. This lattice is currently adopted as the baseline lattice for the HALF storage ring. To evaluate the performance of this lattice, three other HMBA lattices are designed and compared with the HALF H6BA lattice. The remainder of this paper is organized as follows: In Sect. 2, the design of three different HMBA lattices with the same energy and number of lattice cells and similar lengths as HALF is described, and their storage ring properties are compared with the present HALF H6BA lattice. Because the beam energy of HALF is relatively low and its circumference is relatively large, there is significant intra-beam scattering (IBS). Thus, in Sect. 3, we present a study of the IBS effects in these HMBA lattices. Finally, the conclusions are presented in Sect. 4.

2 Lattice design and comparison

We present the design studies of three different HMBA lattices for the HALF storage ring with a beam energy of 2.2 GeV and 20 identical cells comprising a ESRF-EBS type H7BA lattice, the H7BA lattice with RBs, and a Diamond-II-type H6BA lattice, which are compared with the present modified H6BA lattice of HALF.

2.1 Optimization method

In the linear optics design of these three HMBA lattices, a multi-objective genetic algorithm (MOGA) [26] was used with various magnet parameters as the variables. The objective functions employed include the natural emittance and integrated sextupole strengths to facilitate the subsequent nonlinear dynamics optimization [23, 27]. To ensure the practicality and dynamic performance of the lattice, some constraints were set in the linear lattice optimization. First, the transverse phase advances between the two dispersion bumps were set close to $(3\pi, \pi)$ to approximate the I transformation. Second, the transverse tunes of one lattice cell were set near (2.4, 0.9) so that a fourth-order achromat can be created for normal sextupoles over five identical lattice cells [28]. Third, constraints for the maximum magnet strengths and minimum spaces between the magnets were also set in the optimization. For example, the strengths of the quadrupoles in the high- and low-beta regions were limited to less than 45 T/m and 60 T/m, respectively. The distances between the magnets were no less than 0.10 m, and some spaces were also reserved for beam position monitors, correctors, photon absorbers, and other equipment. These constraints were also set for the baseline lattice.

Generally, a HMBA lattice incorporates three families of chromatic sextupoles (SD1, SF, and SD2) in the dispersion bumps for chromaticity correction and nonlinear dynamics optimization. Owing to the specific values of the phase advances between the sextupoles and control over the sextupole strengths and natural chromaticities, the solutions generated from the linear optics optimization of these lattices generally exhibit relatively good nonlinear dynamic performance. After the horizontal and vertical chromaticities were corrected to (+3, +3), we used the OPA code [29] to further optimize the nonlinear dynamics of these lattices mainly by controlling the higher-order chromaticities and

the resonance driving and detuning terms. The optimization knobs included the strengths and positions of the sextupoles and one family of octupoles located in the dispersion bumps. The octupoles can be used to effectively adjust both the amplitude- and momentum-dependent tune shifts [30]. For the present baseline lattice, an additional family of weak sextupoles (SH) integrated with corrector coils was placed in the middle part to optimize its nonlinear dynamics.

2.2 Linear optics and storage ring parameters

The first designed HMBA lattice (denoted as H7BA_1) follows the ESRF-EBS H7BA lattice. To achieve a moderate spacing between the elements, the cell length of this lattice was set to approximately 22 m with a straight section of 5.6 m. The circumference of the designed storage ring is 441.6 m, which corresponds to a harmonic number of 736 at a RF frequency of 500 MHz. After MOGA optimization, a lattice solution with a natural emittance of 84.2 pm rad was selected. Its linear optics and magnet layout are shown in Fig. 1a. Table 1 lists the main storage ring parameters of this and the other HMBA lattices. The energy loss per turn is quite small (118.6 keV for the bare lattice) owing to the weak dipole field. Consequently, the natural damping times are very long, which results in a very significant IBS effect causing a significant emittance increase. The IBS effect is calculated in the next section.

The second lattice (H7BA_2) is also a H7BA lattice with the same cell and straight section lengths as H7BA_1. In contrast to H7BA_1, a pair of RBs is employed in the low-beta region of H7BA_2 to reduce the emittance in a similar manner to the APS-U lattice. As in the HEPS lattice, the central combined-function bend is replaced by an LGB, which is unfavorable for achieving a large horizontal damping partition number (J_x) but provides a better bend radiation source. The LGB consists of three slices with a maximum dipole field of 0.9 T. The selected H7BA_2 lattice solution shown in Fig. 1b has a natural emittance of 71.5 pm rad. The dipole and quadrupole fields of the RB (offset quadrupole) are −0.22 T and 47.7 T/m, respectively.

Figure 2a shows the change of $\varepsilon_{\mathrm{nat}}(s) = C_{\mathrm{q}}\gamma^2 \int^s \mathrm{d}s' H(s')h^3(s')/(J_x \cdot I_2)$ along one lattice

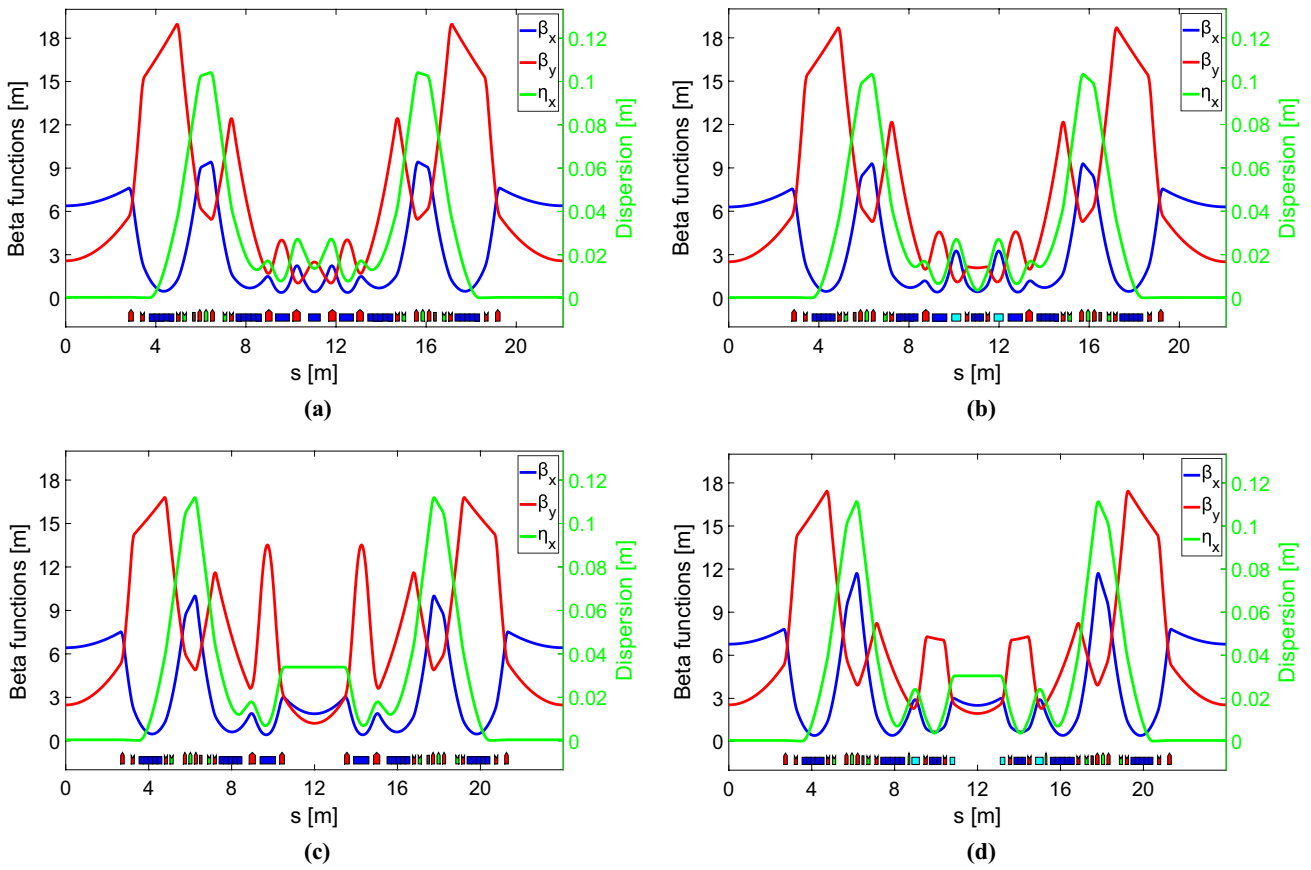

Fig. 1 (Color online) Linear optical functions and magnet layout of the H7BA_1 (**a**), H7BA_2 (**b**), H6BA_1 (**c**) and H6BA_2 (**d**) lattices. In the magnet layout, the bends are shown as blue and cyan (RBs) blocks, and the quadrupoles, sextupoles, and octupoles as red, green and brown blocks, respectively

Table 1 Main storage ring parameters of the four HMBA lattices

Parameter	H7BA_1	H7BA_2	H6BA_1	H6BA_2
Energy (GeV)	2.2			
Circumference (m)	441.6	441.6	479.86	479.86
Number and lengths of straight sections	20×5.6 m	20×5.6 m	$20 \times (5.3 + 2.9)$ m	$20 \times (5.3 + 2.2)$ m
Straight section ratio	25.4%	25.4%	34.2%	31.3%
Natural emittance (pm rad)	84.1	71.5	103.3	85.8
Betatron tunes (H/V)	48.17/17.17	48.17/17.17	48.19/17.19	48.19/17.19
Natural chromaticities (H/V)	$-72/-59$	$-75/-60$	$-72/-75$	$-82/-57$
Momentum compaction	1.73×10^{-4}	1.31×10^{-4}	1.59×10^{-4}	0.94×10^{-4}
Natural energy spread	5.43×10^{-4}	6.09×10^{-4}	5.18×10^{-4}	6.07×10^{-4}
Energy loss per turn (bare) (keV)	118.6	157.5	122.9	181.4
Natural damping times ($H/V/E$) (ms)	36.4/54.6/36.4	26.3/41.2/28.7	43.9/57.3/33.8	28.5/38.8/23.7
Damping partition numbers ($H/V/E$)	1.5/1/1.5	1.57/1/1.43	1.31/1/1.69	1.36/1/1.64
Total absolute bending angle (°)	360	415.9	360	438.6
β_x/β_y at the long straight section (m)	6.4/2.6	6.3/2.5	6.4/2.5	6.8/2.5
β_x/β_y at the short straight section (m)	–	–	1.9/1.2	2.5/1.9

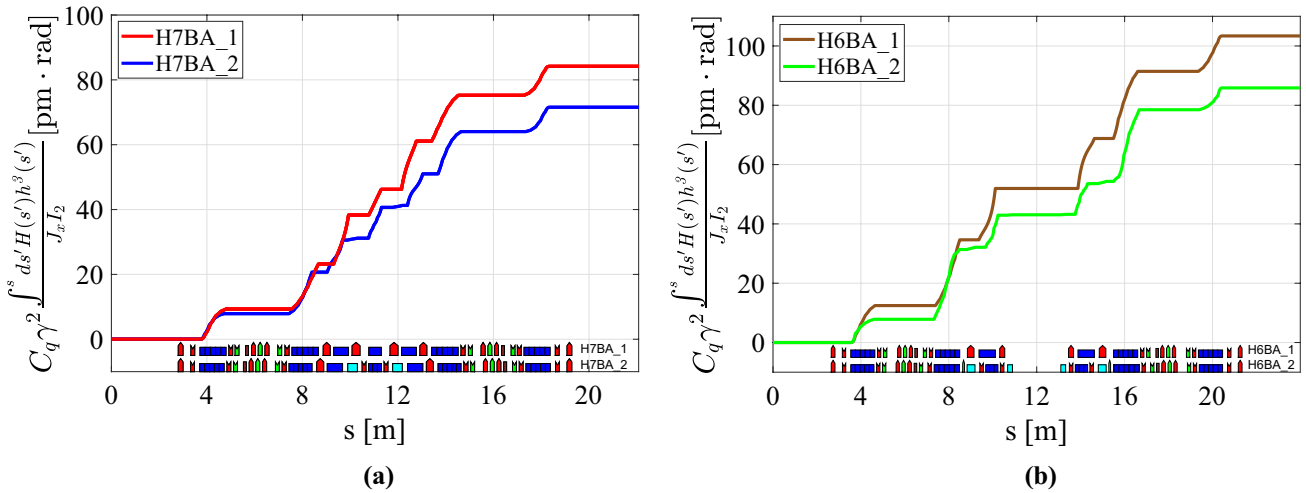

Fig. 2 (Color online) Change of $\varepsilon_{\mathrm{nat}(s)}$ along one cell in the four HMBA lattices. **a** H7BA_1 and H7BA_2; **b** H6BA_1 and H6BA_2

cell in H7BA_1 and H7BA_2 where $C_q = 3.83 \times 10^{-13}$ m, γ is the electron Lorentz factor, $I_2 = \oint h^2(s)\mathrm{d}s$ the radiation integral, H the dispersion invariant, and h the bending curvature. $\varepsilon_{\mathrm{nat}}(s)$ reflects the contribution of each bend to the quantum excitation (excluding the effects of J_x and I_2). Compared to H7BA_1, the RBs used in H7BA_2 help reduce the quantum excitation from the adjacent main bends. In addition, the use of a RB, which increases the total absolute bending angle, and a LGB with an inhomogeneous dipole field can increase the radiation loss and thus reduce the damping times, which helps to suppress the IBS effect. Compared to H7BA_1, the emittance of H7BA_2 is reduced by approximately 15%. This reduction is not as obvious in the APS-U lattice. This is mainly because a RB was not placed in the dispersion bump region of the H7BA_2 lattice so that the quadrupole fields can be adjusted more flexibly for optical compensation when IDs are inserted in the HALF storage ring. In addition, the central LGB replacing the combined-function bend has no quadrupole field. Thus, the J_x of H7BA_2 is only slightly larger than that of H7BA_1 and lower than that of APS-U. The emittance of H7BA_2 can be further reduced by using more RBs and a larger J_x.

The third lattice (H6BA_1) is a Diamond-II type H6BA lattice. The primary advantage of this lattice is that the number of straight ID sections can be doubled. The current baseline lattice of HALF also has long and short straight

sections in each lattice cell. To provide a better comparison, the lengths of the lattice cell and long straight section of H6BA_1 were set to 23.993 and 5.3 m, respectively, to match those of the HALF baseline lattice. The ring circumference is 479.86 m with a harmonic number of 800 for a RF frequency of approximately 500 MHz. Figure 1c shows the designed H6BA_1 lattice, which has a natural emittance of 103.3 pm rad. Compared to H7BA_1, the J_x of H6BA_1 is smaller by more than 10% and the natural emittance larger by more than 20% owing to the absence of a central combined-function bend. The vertical natural chromaticity of H6BA_1 is nearly 30% larger than that of H7BA_1 owing to the larger vertical beta functions, which may result in relatively stronger sextupoles and significant nonlinear dynamics. In this lattice, the length of the short straight section is 2.9 m. The ratio of the total length of the long and short straight sections to the cell length is approximately 34%, which is comparable to that of third-generation light sources. Note that because IDs located in short straight sections may influence the phase advances for nonlinear dynamics cancellation, the peak field should not be too large, and careful compensation may be required.

The fourth lattice (H6BA_2) is the baseline HALF lattice, which is the modified H6BA lattice proposed in Ref. [15, 31]. In contrast to the H6BA_1 lattice, LGB/RB unit cells are used in the central part of this lattice. This can reduce both the emittance and damping times at the cost of a decrease in the momentum compaction factor and the length of the short straight section. The short straight section length of H6BA_2 is 2.2 m and the straight section ratio is approximately 31%. In addition, the change in the dipole field of the second LGB in H6BA_2 is nonmonotonic owing to the effect of the adjacent RB. Figure 1d shows the H6BA_2 lattice. Figure 2b shows the change in $\varepsilon_{\mathrm{nat}}(s)$ along one lattice cell in the H6BA_1 and H6BA_2 lattices. The LGB/RB unit cell provides a lower emittance increase than the combined-function bend unit cell. From Table 1, it can be seen that, overall, the damping time of the H6BA_2 lattice is shorter than those of the others, and the H6BA_2 lattice has nearly the same natural emittance as the H7BA_1 lattice.

2.3 Nonlinear dynamics performance

Careful control and optimization of the nonlinear dynamics are required to increase the injection efficiency and beam lifetime of the storage ring. The integrated strengths of the sextupoles and octupoles used in these four lattices were obtained after nonlinear dynamic optimization with the same expression as that in the OPA code and listed in Table 2. The nonlinear magnets of the four HMBA lattices are relatively weak. Figure 3 shows the on-momentum 4D DAs and DAs with the RF cavity and synchrotron radiation included in these four lattices (without considering errors). In general, the two H7BA lattices have slightly larger DAs than the two H6BA lattices. Compared to the 4D DAs, the DAs with the RF cavity and synchrotron radiation are approximately 30% smaller in the horizontal plane. This is because the path length of on-momentum particles at large transverse amplitudes is longer than the nominal value, resulting in considerable longitudinal oscillation [17]. In the four HMBA lattices, the horizontal DAs in the positive direction are larger than those in the negative direction. To evaluate the robustness, random magnet errors were included to generate residual error effects (without correction) such as orbit distortions and beta-beating of a few percents; multipole field errors were also added. With these errors and the physical

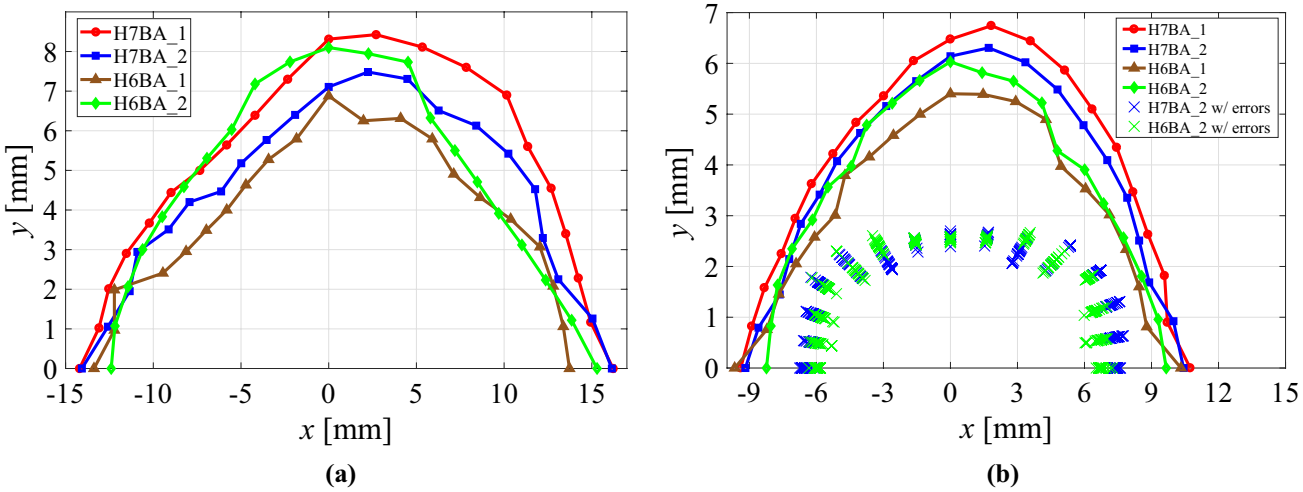

Fig. 3 (Color online) On-momentum 4D DAs (**a**) and DAs with RF cavity and synchrotron radiation included (**b**) of the four HMBA lattices at the middle of the long straight section

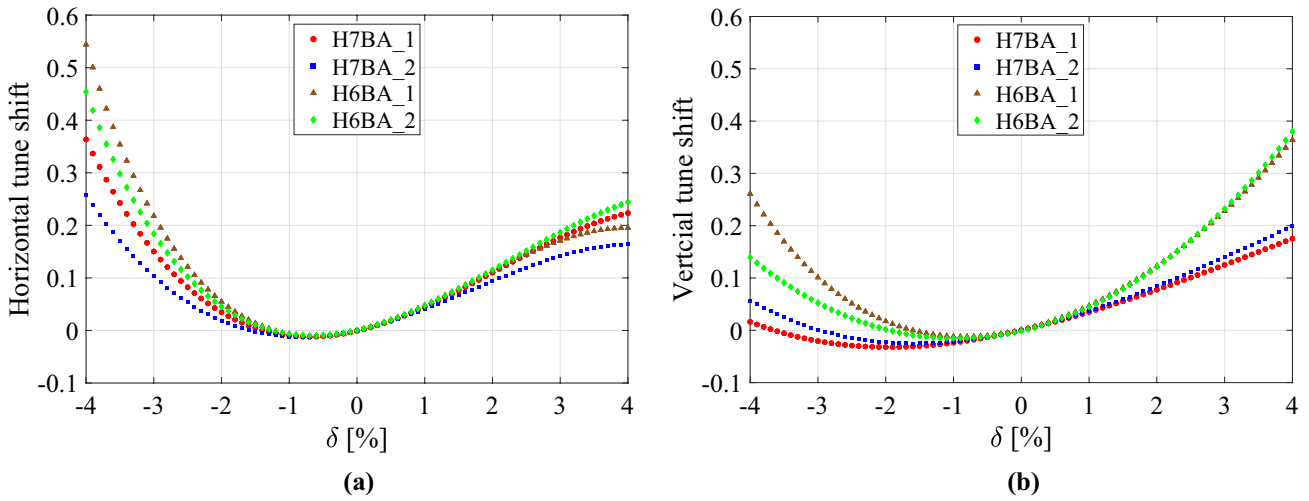

Fig. 4 (Color online) Variation of horizontal (**a**) and vertical (**b**) tune shifts with momentum in the four HMBA lattices

Table 2 Integrated sextupole and octupole strengths of the four HMBA lattices

	H7BA_1	H7BA_2	H6BA_1	H6BA_2
b_3L of SD1 (m^{-2})	−14.11	−15.48	−17.67	−14.50
b_3L of SF (m^{-2})	18.06	18.69	17.74	19.79
b_3L of SD2 (m^{-2})	−14.10	−14.87	−14.41	−18.35
b_3L of SH (m^{-2})	–	–	–	0.30
b_4L of octupole (m^{-3})	−130	−180	−190	−200

aperture included, the horizontal DA (rms value) is reduced to approximately −6.5–7.4 mm for the H7BA_2 lattice and approximately −6.0–6.8 mm for the H6BA_2 lattice, as shown in Fig. 3b. Similar nonlinear dynamics performance can be expected for the other two lattices with the errors included. Nevertheless, the horizontal DAs of these lattices are compatible with the off-axis injection scheme. Figure 4 shows the momentum-dependent tuning shifts. The two H6BA lattices generally exhibit larger tune shifts in both planes than the two H7BA lattices.

The lifetime of a DLSR is generally dominated by Touschek scattering [32], which refers to large collisions between electrons inside a bunch with the transfer of transverse momentum to longitudinal momentum. Particle loss occurs when the longitudinal momentum exceeds the acceptance. For a storage ring with a fixed beam energy, the Touschek lifetime is mainly influenced by the momentum aperture (MA) along the entire storage ring and the electron bunch density. To evaluate the Touschek lifetimes of the four lattices, their local MAs were tracked and the results shown in Fig. 5. During tracking, the RF voltage was set to achieve an energy acceptance of approximately 5% for each lattice. The minimum local MA was approximately 3% at the dispersion bumps. To increase

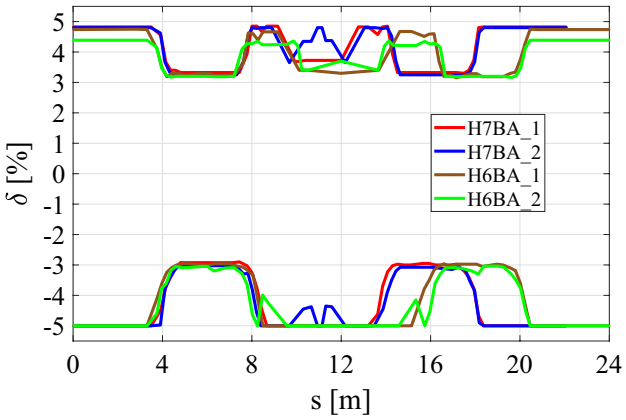

Fig. 5 (Color online) Local MAs of the four HMBA lattices along one cell

the lifetime, the bunch length was assumed to be moderately increased by a factor of three, which can be achieved by using a one-cell superconducting passive harmonic cavity [33]. Using these settings, the Touschek lifetimes were calculated for the four lattices. Assuming that 80% of the buckets are equally filled with bunches, a bunch charge of 1 nC corresponds to a beam current of 400 mA in HALF. In this case, the Touschek lifetimes of these four lattices are greater than 8 and 17 h at the transverse coupling ratios of 10 and 100%, respectively. With error effects considered, the Touschek lifetimes are reduced by approximately 30–40% in the H6BA_2 lattice.

3 IBS effect

IBS refers to the small-angle multiple scattering of charged particles, which does not result in particle loss but changes the beam dimensions and increases the equilibrium emittance [34]. For the HALF storage ring, which has ultra-low natural emittance and relatively low beam energy, the IBS effect is a severe problem that limits the performance of HALF, for example in terms of its photon beam brightness and transverse coherence. There are two main approaches to mitigate the IBS effect in a DLSR with a fixed beam energy. First, the bunch density can be reduced to suppress emittance growth. This can be achieved by increasing the bunch length using a harmonic cavity and increasing the transverse coupling factor. Round beam operation is therefore considered for the HALF storage ring, which can be achieved by driving a linear difference coupling resonance [35]. The second approach is to reduce the damping time by increasing the radiation loss, which can be achieved by employing LGBs and RBs in the lattice design and adding damping wigglers in the dispersion-free straight sections.

To estimate the IBS effects in the four designs, we calculated the equilibrium emittance and energy spread for different bunch charges and show the results in Fig. 6. In the calculation, the settings for the RF cavity were set to those used in the Touschek lifetime calculation, and the bunch length was assumed to be lengthened by a factor of three to mitigate the IBS effect. For round beam operation with a bunch charge of 1 nC, the horizontal (vertical) emittances of the H7BA_1, H7BA_2, H6BA_1, and H6BA_2 lattices are 99.9, 84.4, 117.5, and 92.0 pm rad, respectively, which are 98%, 93%, 101% and 86% larger than their zero current cases. The round beam emittance was calculated as $\varepsilon_x = \varepsilon_y = \varepsilon_0 \cdot J_x/(J_x + 1)$.

Damping wigglers can be employed to further reduce the equilibrium emittance by providing additional radiation damping. This approach has been used in PETRA-IV and NSLS-II [18, 36]. Generally, a damping wiggler with a shorter period favors emittance reduction while a higher dipole field favors enhanced radiation damping. It is intended that two damping wigglers will be employed in the HALF storage ring. Each wiggler consists of 42 periods with a period length of 100 mm and a peak dipole field of 1.9 T. Table 3 lists some storage ring parameters of the four lattices with the two damping wigglers added. We observed that the radiation loss is increased by approximately 93 keV. The vertical damping times are reduced by 33–44% and the J_x values reduced by 8–15%. The equilibrium emittance and energy spread at different bunch charges with the damping

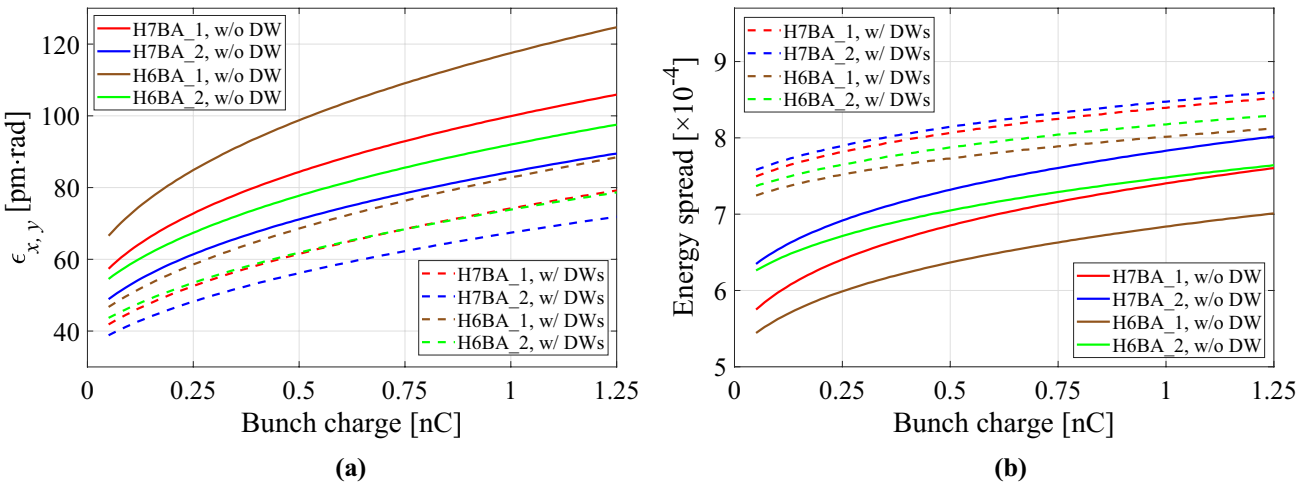

Fig. 6 (Color online) Equilibrium emittance (**a**) and energy spread (**b**) values at different bunch charges at the transverse coupling ratio of 100% (without damping wigglers and IDs)

Table 3 Some storage ring parameters of the four lattices with damping wigglers added, where $\varepsilon_{\mathrm{IBS,DW}}$ is the equilibrium emittance for round beam operation with a bunch charge of 1 nC

Parameter	H7BA_1	H7BA_2	H6BA_1	H6BA_2
Energy loss per turn (keV)	211.5	250.4	215.8	274.3
Damping times (*H*/*V*/*E*) (ms)	23.9/30.6/17.8	19.1/25.9/15.7	27.8/32.6/17.9	20.7/25.7/14.6
J_x	1.28	1.36	1.17	1.24
Energy spread	7.37×10^{-4}	7.45×10^{-4}	7.14×10^{-4}	7.26×10^{-4}
$\varepsilon_{\mathrm{IBS,DW}}$ (pm rad)	74.2	67.4	83.3	73.9

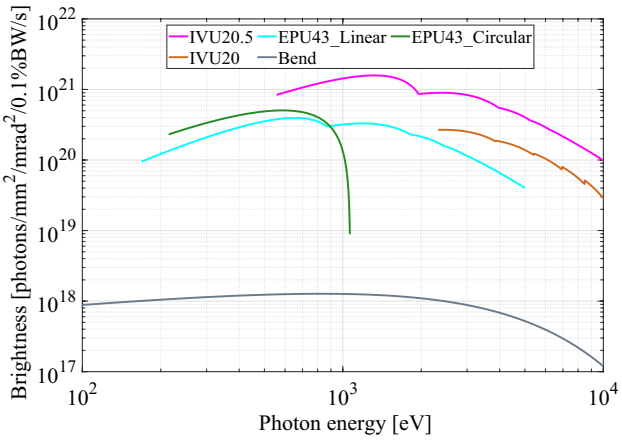

Fig. 7 (Color online) Brightness curve for the IDs and 0.9 T bends of HALF with the H6BA_2 lattice. The IVU20.5 and EPU43 with lengths of 4.1 m are installed in the long straight sections, and the IVU20 with a length of 1.5 m is installed in the short straight section

wigglers added are shown in Fig. 6. At the bunch charge of 1 nC, the round beam equilibrium emittances for the H7BA_1, H7BA_2, H6BA_1, and H6BA_2 lattices are 74.2, 67.4, 83.3, and 73.9 pm rad, respectively. The emittance growth due to the IBS effect is relatively weak in ALS-U [13]. This can probably be attributed to the relatively long bunch length and short damping time. The equilibrium emittance of HALF can be further reduced if IDs are included or if the bunch length is further increased.

The H7BA_2 and H6BA_2 lattices exhibit lower equilibrium emittances than the other two HMBA lattices. The radiation properties of the H7BA_2 lattice are slightly superior to those of the H6BA_2 lattice; however, the latter has 20 additional straight sections. Although the IDs in these straight sections are shorter (approximately 1.5 m), their radiation brightness is much higher than that of the bends. Figure 7 shows the brightness curve for HALF with the H6BA_2 lattice. The IVU20 is an in-vacuum undulator with a period length of 20 mm, total length of 1.5 m, and peak dipole field of 1.06 T, which is installed in the short straight section. The brightness of soft X-rays from the IVU20 is larger than 10^{20} photons/mm^2/mrad^2/0.1%BW/s, which is generally higher than the ID radiation within the same wave range in third-generation light sources. Therefore, a H6BA_2 lattice with long and short straight sections is more attractive to the NSRL user community.

We next summarize the characteristics of the four HMBA lattices designed for HALF. Although the nonlinear dynamics characteristics of the two H7BA lattices are superior to those of the two H6BA lattices with additional short straight sections, all four lattices have relatively large DAs and moderate MAs that provide for off-axis injection and reasonable Touschek lifetimes. From the equilibrium emittance point of view, the H7BA_2 and H6BA_2 lattices have lower equilibrium emittances and relatively short damping times for suppressing IBS-induced emittance growth. Considering the straight sections, the two H6BA lattices have more straight sections to accommodate high-brightness IDs. Because the equilibrium emittance and number of straight sections are the two most important parameters for users, the H6BA_2 lattice is preferred for HALF.

4 Conclusion

In this study, three types of HMBA lattices comprising the ESRF-EBS type H7BA lattice, the H7BA lattice with RBs, and the Diamond-II type H6BA lattice were designed for the HALF storage ring with a beam energy of 2.2 GeV and 20 identical cells. The main storage ring properties of these three lattices and the present HALF H6BA lattice were compared. The design and comparison results show that with IBS considered, the H7BA lattice with RBs and the present HALF H6BA lattice have smaller equilibrium emittances than those of the other two lattices. The two H7BA lattices have slightly larger on-momentum DAs and smaller momentum-dependent tune shifts than those of the two H6BA lattices. However, the DAs of these four HMBA lattices are sufficiently large for off-axis injection, and the MAs exhibit reasonable Touschek lifetimes. The two H6BA lattices have two straight sections in each cell and can provide more IDs than the two H7BA lattices. Therefore, considering both the equilibrium emittance and number of straight sections, the present H6BA lattice is the best scheme for the HALF storage ring among the four HMBA lattices. To mitigate the significant IBS effect, bunch lengthening with a harmonic cavity, round beam operation, and damping wigglers are adopted in HALF. With these measures, the equilibrium emittance of the HALF 6BA lattice was found to be slightly larger than 70 pm rad. And the emittance will be further reduced by including IDs.

Author contributions All authors contributed to the study conception and design. Material preparation, data collection and analysis were performed by Peng-Hui Yang, Gang-Wen Liu, Jian-Hao Xu, Wei-Wei Li, Tian-Long He and Zheng-He Bai. The first draft of the manuscript was written by Peng-Hui Yang and all authors commented on previous versions of the manuscript. All authors read and approved the final manuscript.

Data availability The data that support the findings of this study are openly available in Science Data Bank at https://doi.org/10.57760/sciencedb.j00186.00089 and https://cstr.cn/31253.11.sciencedb.j00186.00089

Declarations

Conflict of interest The authors declare that they have no competing interests.

References

1. W. Xu, D. Jia, S.P. Jiang et al., Upgrade project on top-off operation for Hefei light source, in *Proceedings of the IPAC 2017*, vol 2017 (Copenhagen, Denmark) (2017), pp. 2719–2722. https://doi.org/10.18429/JACoW-IPAC2017-WEPAB064
2. L. Wang, W.M. Li, G.Y. Feng et al., The upgrade project of Hefei light source (HLS), in *Proceedings of the IPAC 2010* (Kyoto, Japan, 2010), pp. 2588–2590
3. J.Y. Li, G. Huang, W. Wei et al., Operational status of HLS-II, in *Proceedings of the IPAC 2016* (Busan, Korea, 2016), pp. 4155–4158. https://doi.org/10.18429/JACoW-IPAC2016-THPOY028
4. C.F. Wu, L. Wang, C. Li et al., The 4th harmonic cavity for Heifei Light Source-II, in *Proceedings of the IPAC 2016* (Busan, Korea, 2016), pp. 837–839. https://doi.org/10.18429/JACoW-IPAC2016-MOPOW054
5. Z. Ren, B. Wei, H. Xu et al., Modified double-double bend achromat lattice for an ultra-low emittance design of the HLS. J. Instrum. **17**, P07001 (2022). https://doi.org/10.1088/1748-0221/17/07/p07001
6. R. Hettel, DLSR design and plans: an international overview. J. Synchrotron Radiat. **21**, 843–855 (2014). https://doi.org/10.1107/S1600577514011503
7. P.F. Tavares, S.C. Leemann, M. Sjostrom et al., The MAX IV storage ring project. J. Synchrotron Radiat. **21**, 862–877 (2014). https://doi.org/10.1107/S1600577514011515
8. P. Raimondi, N. Carmignani, L.R. Carver et al., Commissioning of the hybrid multibend achromat lattice at the European synchrotron radiation facility. Phys. Rev. Accel. Beams **24**, 110701 (2021). https://doi.org/10.1103/PhysRevAccelBeams.24.110701
9. L. Liu, N. Milas, A.H.C. Mukai et al., The sirius project. J. Synchrotron Radiat. **21**, 904–911 (2014). https://doi.org/10.1107/S1600577514011928
10. M. Borland, T.G. Berenc, R.R. Lindberg et al., Lower emittance lattice for the advanced photon source upgrade using reverse bending magnets, in *Proceedings of the NAPAC 2016* (Chicago, IL, USA, 2016), pp. 877–880. https://doi.org/10.18429/JACoW-NAPAC2016-WEPOB01
11. Y. Jiao, G. Xu, X. Cui et al., The HEPS project. J. Synchrotron Radiat. **25**, 1611–1618 (2018). https://doi.org/10.1107/S1600577518012110
12. A. Streun, T. Garvey, L. Rivkin et al., SLS-2-the upgrade of the Swiss Light Source. J. Synchrotron Radiat. **25**, 631–641 (2018). https://doi.org/10.1107/S1600577518002722
13. C. Steier, A.P. Allézy, A. Anders et al., Status of the conceptual design of ALS-U, in *Proceedings of the IPAC 2018* (Vancouver, BC, Canada, 2018), pp. 4134–4137. https://doi.org/10.18429/JACoW-IPAC2018-THPMF036
14. E. Karantzoulis, W. Barletta, Aspects of the Elettra 2.0 design. Nucl. Instrum. Methods Phys. Res. A **927**, 70–80 (2019). https://doi.org/10.1016/j.nima.2019.01.044
15. Z.H. Bai, G.Y. Feng, T.L. He et al., A modified hybrid 6BA lattice for the HALF storage ring, in *Proceedings of the IPAC 2021* (Campinas, SP, Brazil, 2021), pp. 407–409. https://doi.org/10.18429/JACoW-IPAC2021-MOPAB112
16. D. Einfeld, J. Schaper, M. Plesko, Design of a diffraction limited light source (DIFL), in *Proceedings of the PAC, Dalls, USA, TPG08* (1995), pp. 177–179. https://doi.org/10.1109/PAC.1995.504602
17. J.C. Biasci, J.F. Bouteille, N. Carmignani et al., A low-emittance lattice for the ESRF. Synchrotron Radiat. News **27**(6), 8–12 (2014). https://doi.org/10.1080/08940886.2014.970931
18. C.G. Schroer, I. Agapov, W. Brefeld et al., PETRA IV: the ultralow-emittance source project at DESY. J. Synchrotron Radiat. **25**, 1277–1290 (2018). https://doi.org/10.1107/S1600577518008858
19. C. Sun, H. Nishimura, D. Robin et al., Optimization of the ALS-U storage ring lattice, in *Proceedings of the IPAC 2016* (Busan, Korea, 2016), pp. 2959–2961. https://doi.org/10.18429/JACoW-IPAC2016-WEPOW050
20. A. Alekou, P. Raimondi, R. Bartolini et al., Study of double triple bend achromat (DTBA) lattice for a 3GeV light source, in *Proceedings of the IPAC 2016* (Busan, Korea, 2016), pp. 2940–2942. https://doi.org/10.18429/JACoW-IPAC2016-WEPOW044
21. X.Z. Liu, S.Q. Tian, X. Xu et al., Intra-beam scattering and beam lifetime in a candidate lattice of the soft X-ray diffraction-limited storage ring for the upgraded SSRF. Nucl. Sci. Tech. **32**, 83 (2021). https://doi.org/10.1007/s41365-021-00913-y
22. Y. Zhao, Y. Jiao, S. Wang, Design study of APS-U-type hybrid-MBA lattice for mid-energy DLSR. Nucl. Sci. Tech. **32**, 71 (2021). https://doi.org/10.1007/s41365-021-00902-1
23. P. Yang, Z. Bai, T. Zhang et al., Design of a hybrid ten-bendachromat lattice for a diffraction-limited storage ring light source. Nucl. Instrum. Methods Phys. Res. A **943**, 162506 (2019). https://doi.org/10.1016/j.nima.2019.162506
24. A. Loulergue, P. Alexandre, P. Brunelle et al., Baseline lattice for the upgrade of SOLEIL, in *Proceedings of the IPAC 2018* (Vancouver, BC, Canada, 2018), pp. 4726–4729. https://doi.org/10.18429/JACoW-IPAC2018-THPML034
25. J. Xu, Z. Ren, P. Yang et al., A seven-bend-achromat lattice option for the HALF storage ring. J. Instrum. **17**(01), P01001 (2022). https://doi.org/10.1088/1748-0221/17/01/p01001
26. K. Deb, A. Pratap, S. Agarwal et al., A fast and elitist multiobjective genetic algorithm: NSGA-II. IEEE Trans. Evol. Comput. **6**(2), 182–197 (2002). https://doi.org/10.1109/4235.996017
27. P. Yang, Z. Bai, J. Xu et al., Comparison of optimization methods for hybrid seven-bend-achromat lattice design. J. Phys. Conf. Ser. **1350**(1), 012031 (2019). https://doi.org/10.1088/1742-6596/1350/1/012031
28. K.L. Brown, A second-order magnetic optical achromat. IEEE Trans. Nucl. Sci. **26**(3), 3490–3492 (1979). https://doi.org/10.1109/TNS.1979.4330076
29. A. Streun, OPA version 3.39 PSI (2014)
30. S.C. Leemann, A. Streun, Perspectives for future light source lattices incorporating yet uncommon magnets. Phys. Rev. Accel. Beams **14**, 030701 (2011). https://doi.org/10.1103/PhysRevSTAB.14.030701
31. Z. Bai, Lattice design progress of the HALF storage ring, in *3rd workshop on low emittance lattice design* (Barcelona, Spain, 2022). https://indico.cells.es/event/1072/contributions/1857/
32. A. Piwinski, The Touschek effect in strong focusing storage rings. Cern Library Record (1999). https://arxiv.org/pdf/physics/9903034.pdf
33. T. He, Z. Bai, W. Li et al., Bunch lengthening of the HALF storage ring in the presence of passive harmonic cavities, in *Proceedings of the IPAC 2021* (Campinas, SP, Brazil, 2021), pp. 2082–2085. https://doi.org/10.18429/JACoW-IPAC2021-TUPAB265
34. A. Piwinski, Intra-beam-scattering (1974)
35. C.C. Du, J.Q. Wang, D.H. Ji et al., Studies of round beam at HEPS storage ring by driving linear difference coupling resonance. Nucl. Instrum. Methods Phys. Res. A **976**, 164264 (2020). https://doi.org/10.1016/j.nima.2020.164264
36. W. Guo, S. Kramer, S. Krinsky et al., NSLS-II lattice optimization with damping wigglers, in *Proceedings of the PAC 2009* (Vancouver, BC, Canada, 2009), pp. 1102–1104. https://accelconf.web.cern.ch/PAC2009/papers/tu5rfp008.pdf